Observation of proportionality between friction and contact area at the nanometer scale

M. Enachescu *, R.J.A. van den Oetelaar, R.W. Carpick **, D.F. Ogletree, C.F.J. Flipse *** and M. Salmeron +

Materials Sciences Division, Lawrence Berkeley National Laboratory, University of California, Berkeley, CA 94720, USA
E-mail: salmeron@stm.lbl.gov

The nanotribological properties of a hydrogen-terminated diamond(111)/tungsten-carbide interface have been studied using ultra-high vacuum atomic force microscopy. Both friction and local contact conductance were measured as a function of applied load. The contact conductance experiments provide a direct and independent way of determining the contact area between the conductive tungsten-carbide AFM tip and the doped diamond sample. We demonstrate that the friction force is directly proportional to the real area of contact at the nanometer-scale. Furthermore, the relation between the contact area and load for this extremely hard heterocontact is found to be in excellent agreement with the Derjaguin–Müller–Toporov continuum mechanics model.

Keywords: nanotribology, friction, contact area, atomic force microscopy, diamond, tungsten carbide

1. Introduction

According to the classical law of friction, the friction force between two bodies in motion is proportional to the applied load and independent of the apparent area of contact [1]. However, a macroscopic contact between two apparently flat solid surfaces consists in practice of a large number of micro-contacts between the asperities that are present on both contacting surfaces. The classical law of friction, which cannot be understood or deduced from first principles, is the result of many complex phenomena at the interface, in particular the specific interactions between contacting asperities, and the corresponding deformations of these asperities [2]. Although macroscopic tribological research can provide important empirical information about the frictional behavior of materials, it cannot explain friction at a fundamental level. Only detailed studies of friction at a single-asperity contact, under well-defined conditions and with nanometer-scale or even atomic-scale resolution, can result in an understanding of friction at a fundamental level. Recent ultra-high vacuum atomic force microscopy (UHV-AFM) experiments indicate that friction is proportional to the contact area for a nanometer-sized single-asperity contact [3–6]. In some of these studies, the contact area was not directly measured but instead derived from continuum mechanics models, although, as discussed further below, it is generally not clear *a priori* which model is valid for a specific combination of materials. As well, most of these experiments were performed on layered materials, where it is unclear whether continuum mechanics models can be used quantitatively. Nevertheless, the continuum mechanics models generally provided convincing fits to the data. Carpick et al. [3] performed experiments on muscovite mica and found that friction was proportional to the contact area as described by the Johnson–Kendall–Roberts (JKR) model [7]. Experiments by Lantz et al. [4] on $NbSe_2$ and graphite resulted in a relation between friction and contact area as described by the Maugis–Dugdale (MD) model [8]. Only one observation of the Derjaguin–Müller–Toporov (DMT) model [9] has been reported so far by Enachescu et al. [5] for an extremely hard heterocontact, involving stiff materials with low adhesive forces, i.e., a tungsten-carbide AFM tip in contact with a hydrogen-terminated diamond(111) sample. Both diamond and tungsten carbide are extremely stiff, non-layered materials. Furthermore, hydrogen passivates the diamond surface while carbides are generally quite inert.

In this paper, we discuss the results of a nanotribological study of a hydrogen-terminated diamond(111)/tungsten-carbide single asperity interface using UHV-AFM. Since the diamond sample is slightly boron-doped and the tungsten-carbide tip is conductive, we are able to measure the local contact conductance as a function of applied load. These experiments provide an independent way of determining the contact area, which can be directly compared to the corresponding friction force. Diamond and diamond-like films are important coating materials used in a wide variety of tools, hard disks, micro-machines, and aerospace applications. For micro-machine and hard-disk applications in particular, the nanotribological properties are of great importance [10]. Similarly, tungsten carbide plays an important role in several types of hard coatings [11].

* Permanent address: Department of Physics, University of Bucharest, PO Box MG-11, Bucharest, Romania.
** Present address: Sandia National Laboratories, Mailstop 1413, Albuquerque, NM 87185, USA.
*** Department of Physics, Eindhoven University of Technology, 5600 MB Eindhoven, The Netherlands.
+ To whom correspondence should be addressed.

2. Theoretical background

The indication of recent AFM [3–6] and surface forces apparatus [12] experiments is that the friction force F_f varies with the applied load L in proportion to the tip–sample contact area A. Thus, $F_f = \tau A$, where τ is the shear strength, a fundamental interfacial property. In most cases, the relation between A and L is deduced from elastic continuum mechanics models, assuming a sphere (tip) in contact with a flat plane (sample) [13]. However, the correct relation between A and L not only depends on the exact geometry but also upon the strength of the adhesive forces compared to the elastic deformations [8,14–16].

The JKR and DMT models mentioned above have been deduced for two extreme cases, namely for compliant materials with strong, short-range adhesive forces and for stiff materials with small, long-range adhesive forces, respectively. The empirical nondimensional parameter $\mu = (R\gamma^2/E^{*2}z_0^3)^{1/3}$ can be used to determine which of the two continuum mechanics models is most appropriate [15]. In this expression, R is the sphere radius, γ is the work per unit area required to separate tip and surface from contact to infinity, and E^* is a combined elastic modulus, given by the equation $E^* = [(1-\nu_1^2)/E_1+(1-\nu_2^2)/E_2]^{-1}$, where E_1 and E_2 are the Young's moduli, and ν_1 and ν_2 are the Poisson's ratios of the sphere and plane, respectively. Finally, z_0 represents the equilibrium spacing for the interaction potential of the surfaces. If $\mu > 5$, the JKR theory should be valid, while for $\mu < 0.1$, the DMT theory should describe the relation between A and L [15,16]. Neither the JKR nor the DMT limit is appropriate for the intermediate cases ($0.1 < \mu < 5$). As discussed by Greenwood [16], it is difficult to calculate the exact area of contact for the continuum problem. Greenwood obtained a numerical solution using a Lennard-Jones potential and defined the contact edge as the point of maximum adhesive stress. Greenwood's solution closely resembles the Maugis–Dugdale model. In both cases, the variation of contact area with load then appears very close to the *shape* of the JKR curve for values of $\mu > 0.5$. However, the JKR equation does not correctly predict the *actual* contact area, pull-off force, and thus the adhesion energy, unless $\mu > 5$. Therefore, while a measurement of contact area versus load may resemble a JKR curve, quantitative analysis would be uncertain, as it would highly depend on a specific model for the tip–sample interaction potential.

In the case of the DMT model ($\mu < 0.1$), the contact area A varies with the applied load L in a simple fashion:

$$A = \pi \frac{R^{2/3}}{K^{2/3}}(L + 2\pi\gamma R)^{2/3},$$

where $K = \frac{4}{3}E^*$. The pull-off force or critical load L_c is given by $L_c = -2\pi\gamma R$. The value of L_c can be obtained from AFM approach/retract displacements of the cantilever and sample, by measuring the (negative) normal force required to separate tip and sample. We note that the contact area goes to zero at pull-off, in contrast to the JKR model.

The contact radius in AFM experiments is generally in the nanometer range and, consequently, much smaller than the electronic mean free path. In this limit, the contact conductance becomes directly proportional to the contact area, as described by Sharvin's equation for metallic contacts [17]: $G = 3\pi a^2/4\rho l$, where ρ is the resistivity, l is the mean free path of the conduction electrons, and a is the radius of the contact. We stress that this equation is only valid for nanometer-sized contacts, where $l \gg a$. The linear relationship between the contact conductance and contact area is true whether the junction is ohmic, semiconductor-like, etc. For instance, in the case of a metal/semiconductor contact [18], which matches our tip–sample interface, the current is directly proportional to the area of contact, considering a constant metal/semiconductor barrier height and a constant temperature during the experiments. We do not expect to observe the current to change step-wise with load, i.e., the well-known phenomena of quantized conductance occurring at contacts consisting of only a few atoms [19], since in our experiments the contact area will contain too many atoms.

3. Experimental

The experiments were performed in an UHV chamber (base pressure 7×10^{-11} Torr), since even in moderately evacuated chambers the residual oxygen and water vapor may combine with the sliding action to catalyze a phase change on diamond [20]. The UHV chamber is equipped with a home-built AFM [21], low-energy electron diffraction (LEED), and Auger electron spectroscopy (AES). The sample is an artificial type IIb diamond(111) single crystal, which is terminated with hydrogen and slightly boron-doped. The cleaning procedure used, as well as the single-crystal quality, are described in more detail by van den Oetelaar et al. [22]. Figure 1 shows the LEED pattern taken after the cleaning procedure. This clear (1×1) LEED pat-

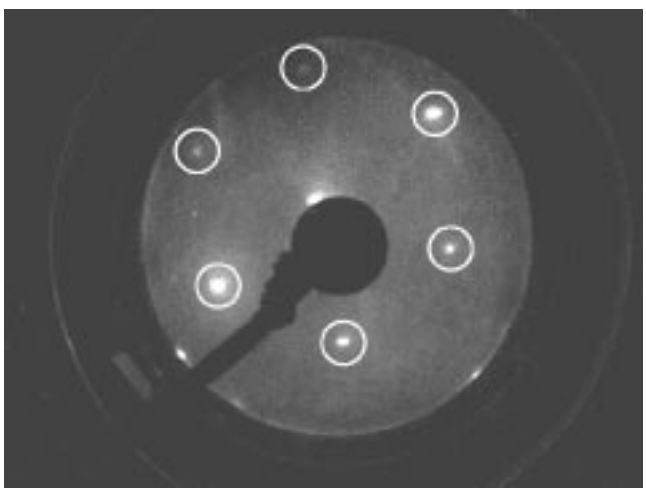

Figure 1. Our cleaning procedure gave rise to a clear hydrogen-terminated diamond(111)-(1×1) surface, as shown in this LEED pattern.

tern supports the fact that we have a hydrogen-terminated diamond(111)-(1×1) surface.

Triangular silicon cantilevers with integrated tips, coated with approximately 20 nm tungsten carbide [23], were used for all measurements. The tips were characterized by scanning electron microscopy (SEM) and AES. Two types of cantilevers were used, with a spring constant of 88 and 0.23 N/m, respectively. The former cantilever was used for conductance measurements while the latter one was used for friction measurements. The tips were cleaned in UHV immediately prior to the measurements, by applying short voltage pulses and/or by rubbing them on the surface. Normal cantilever force constants were taken from the manufacturer, and the normal/lateral force ratio was calculated using the method described by Ogletree et al. [24]. The absolute accuracy of the forces measured is limited due to significant uncertainty in the material properties of the cantilever and approximations used in the force constant calculations. However, relative changes in friction could be accurately determined by using the same cantilever and tip during a series of measurements. A flexible $I-V$ converter, allowing current measurements spanning the range from pA to mA, was designed and built.

Friction versus load data were acquired by scanning the AFM tip repeatedly back and forth over the same line on the surface, while linearly increasing or decreasing the externally applied load. The value of the friction force at a given load is half of the difference between the signals while scanning from left to right, and right to left, respectively [3,25].

4. Results

All of the results presented in this Letter were obtained on a hydrogen-terminated diamond(111) sample, consisting of atomically smooth and well-ordered islands of 150–250 Å in diameter [5,22]. The friction and contact conductance data were acquired within the bounderies of a single island, thus avoiding multiple-contact points.

Figure 2(a) shows a large number of $I-V$ curves recorded at different loads up to 1.7 μN, using an 88 N/m cantilever. The $I-V$ characteristics are semiconductor-like and consistent with the p-type doping of the diamond sample. The shape of the $I-V$ curves remains basically constant at all loads, strongly indicating that the applied load does not significantly affect the surface electronic properties of the interface. This observation supports our assumption that the current is proportional to the contact area.

We can now plot the load dependence of the current at several bias voltages applied to the sample, e.g., 3, 3.5 and 4 V, as is shown in figure 2(b). The data can be fitted by the DMT model, using L_c as a free parameter. The DMT model provides an excellent fit to the measured data, and the value of L_c deduced from the fits is in excellent agreement with the independently measured pull-off force of -0.1 μN, obtained from cantilever–sample retract experiments for the same cantilever.

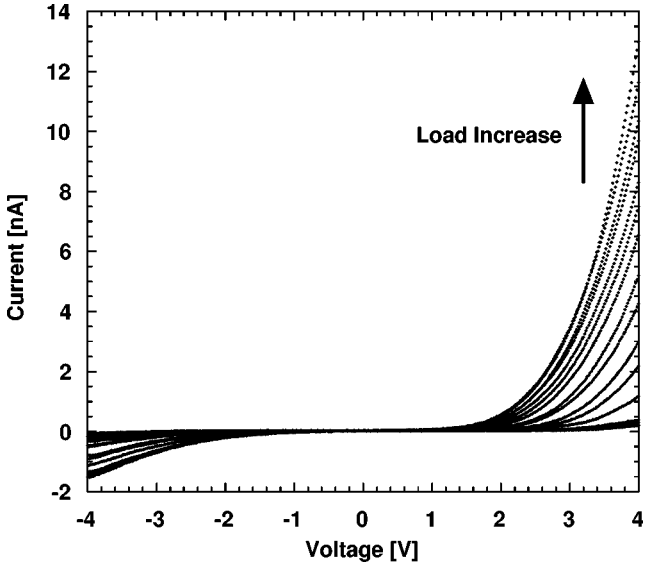

(a)

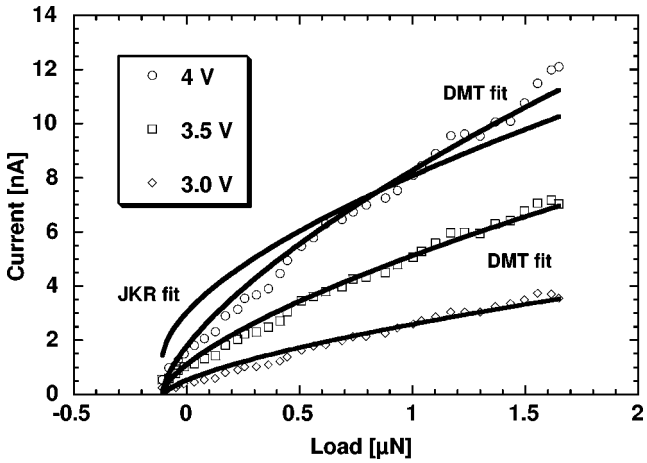

(b)

Figure 2. (a) Current measured through the tip–sample contact versus bias voltage ($I-V$ curves) recorded as a function of increasing load up to 1.7 μN. (b) Current versus applied load at three different constant bias voltages. The DMT fit is significantly better than the JKR fit, as illustrated for a bias voltage of 4 V, also indicated by the mean square deviation of the JKR fit, which is more than one order of magnitude worse for the JKR fit compared to the DMT fit.

We have also tried to fit the current versus load data using the JKR model. Treating L_c as a free parameter, the JKR fits at all bias voltages predict a critical load which is systematically and substantially too small compared to the independently measured pull-off force. If we apply the constraint $L_c = -0.1$ μN to the JKR fit, the resulting fit is clearly incompatible with our data, as illustrated in figure 2(b) for a bias voltage of 4 V. In addition, we found from the fitting statistics that the mean square deviation of the JKR fit is more than one order of magnitude worse than that of the DMT fit. These local contact conductance results clearly show that the load dependence of the contact area for this single-asperity interface can be described by the DMT continuum mechanics model.

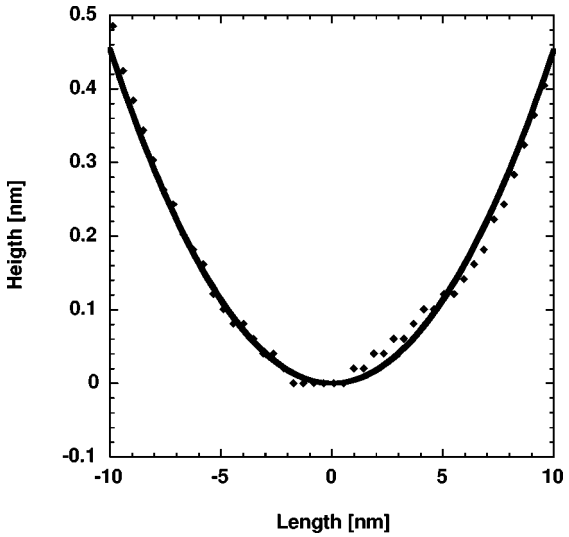

Figure 3. Hemispherical fit of the AFM-tip profile, resulting in a radius of curvature $R = 110$ nm. Note the difference in vertical versus horizontal scale.

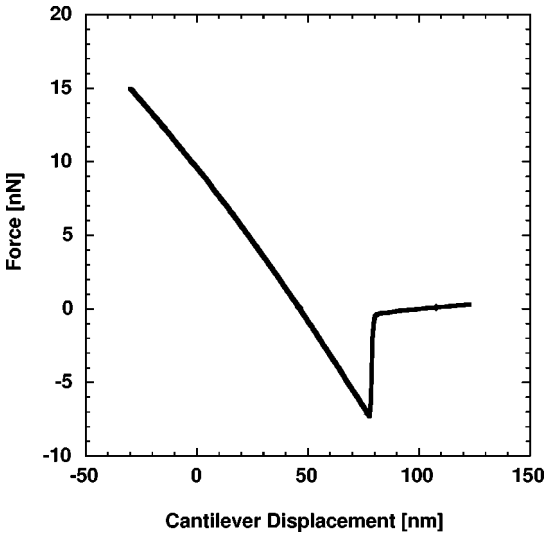

Figure 4. Typical normal force versus cantilever–sample displacement curve, during retraction of the cantilever. The corresponding pull-off force is -7.3 nN.

A topographic AFM image is actually a convoluted image of the tip and surface features of the sample. Usually, one requires sharp AFM tips to reveal the surface topography, but similarly, an extremely sharp feature on the surface can provide information about the shape of an AFM tip [26]. To determine the radius of curvature of the tungsten-carbide-coated tip used in our friction experiments, we performed scans over the sharp edges of a faceted $SrTiO_3$(305) sample [27] in air. The surface is terminated with a large number of (101) and (103) facets, which form long sharp ridges that are suitable for tip imaging [3,24,27]. The thus obtained cross-sectional "image" of the AFM tip actually provides an upper limit to the tip dimensions, but this upper limit appears to be very close to the real tip dimensions [3]. The cross-sectional tip profile can be fitted by a hemisphere, as is shown in figure 3, resulting in a radius of curvature of 110 nm. Profile analysis using the $SrTiO_3$(305) sample was performed before and after tip–sample contact, and no evidence of wear was discerned.

Having obtained a value for the tip radius R, we can estimate the empirical parameter μ. Using $L_c = -2\pi\gamma R$, γ can be obtained from the measured pull-off force. A typical normal force versus cantilever–sample displacement curve, during retraction of the cantilever, is shown in figure 4. The corresponding pull-off force is -7.3 nN, resulting in $\gamma = 0.01$ J/m^2. Thus, using $z_0 = 2$ Å, $E_{\text{diamond}} = 1164$ GPa [28], $E_{\text{WC}} = 700$ GPa [29], $\nu_{\text{diamond}} = 0.08$ [28], and $\nu_{\text{WC}} = 0.24$ [29], we find that $\mu = 0.02$. Indeed, this value is much smaller than the DMT condition $\mu < 0.1$ discussed above, showing that the present tip–sample contact is firmly in the DMT regime.

Friction experiments were performed as a function of applied load using the soft lever [5]. They were reproducible at different locations on the sample, and were obtained by decreasing the load from 12 nN to negative loads (unloading). Experiments where the load was increased (loading) exhibited the same behavior as the unloading results, indicating that the deformation of the contact is elastic for the range of loads investigated.

Friction versus load experiments could be fitted very well by the DMT model, while treating both γ and the shear strength τ as free parameters [5]. The mathematical fit results in a pull-off force of -7.3 nN and a shear strength of 238 MPa. Thus, the pull-off force predicted by the DMT fit is in excellent agreement with the pull-off value measured experimentally, as shown in figure 4. The measured pull-off force actually represents an *independent* verification of the DMT fit, since γ (and thus also the pull-off force) was treated as a free parameter in the DMT fit. Attempts to fit the JKR model to the friction versus load curves, using L_c both as a free parameter and as a constrained parameter, produced strongly inconsistent fits. Experimentally, no friction data for loads smaller than -2 nN could be obtained due to a premature pull-off of the tip. This premature pull-off is promoted by the tip–sample movement during scanning and is more likely to appear in this particular experiment due to the very low adhesive force between the surfaces in contact.

In an attempt to learn more about the relation between the friction force and the area of contact, we have plotted the friction force versus contact area, and the result is shown in figure 5. The friction force plotted in this figure is exactly the friction force measured during friction versus load experiments. The contact area was calculated using the DMT theory. The use of the DMT theory is supported by the three previous pieces of experimental evidence, namely: (i) the excellent DMT fit of the current versus load data using the stiff lever, presented in figure 2(b); (ii) the excellent DMT prediction of the Tabor parameter, $\mu < 0.1$, calculated after experimental determination of the radius of curvature R of the tip presented in figure 3, and of the pull-off force L_c presented in figure 4; (iii) the ex-

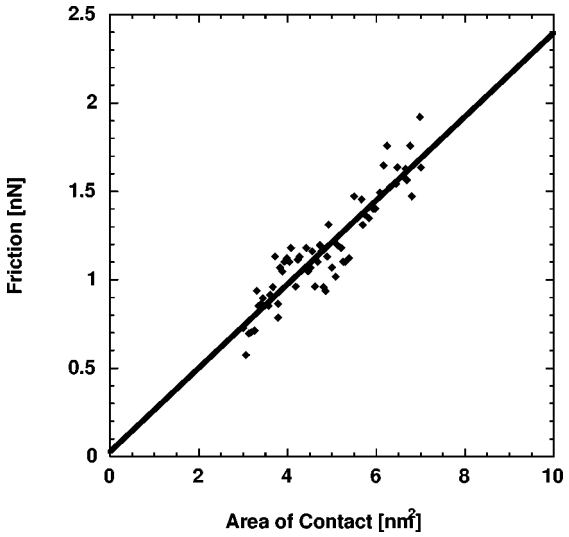

Figure 5. Friction force versus contact area, showing a clear linear relation. The corresponding shear strength $\tau = 238$ MPa.

cellent DMT fit of the friction versus load experiments and the independent confirmation of the DMT fit by the experimental value of L_c presented in figure 4. Following the procedure suggested and supported above we found that a linear fit is the optimum fit for our friction force versus contact area representation in figure 5, demonstrating that, indeed, $F_f = \tau A$. Consistently, this free linear fit intercepts the origin, and the slope is a measure of the shear strength. We find that the shear strength $\tau = 238$ MPa, a value which lies within the typical range for AFM experiments [30].

So, in contrast to the macroscopic law of friction, the friction force at the interface of a single asperity is directly proportional to the contact area. Furthermore, since friction does not depend linearly upon the applied load for a single-asperity contact, one should be careful defining a friction coefficient, i.e., the friction force divided by the normal force, in AFM experiments, as its value varies with load.

The constant shear strength that we observe indicates that the mechanism of energy dissipation for this system does not change in this pressure range. Thus, the increase in friction with load is attributable to the increase in contact area, i.e., more atoms in contact, as opposed to a change in the frictional dissipation per interfacial atom. This may not be so surprising given that the nominal stress is only increasing as roughly $L^{1/3}$ (from the continuum mechanics models). The most likely mechanism of energy dissipation is thermalization of phonons generated at the contact zone during sliding. New modes of energy dissipation, resulting from inelastic processes, may activate at higher stresses [30]. For example, evidence of tip-induced atomic-scale wear has been reported for alkali-halide materials [31]. Pressure-activated modes of energy dissipation are reported in organic thin films due to progressive molecular deformation [32]. These examples represent stress-dependent increases in the number of energy dissipation channels and are therefore manifested in increases in the shear strength compared with purely elastic, wearless friction.

Finally, we comment on the relative magnitude of the observed shear strength. The theoretical prediction for the shear strength of a crystalline material in the absence of dislocations is roughly given by $G/30$ [33], where G is the shear modulus. We can define an "effective" interfacial shear modulus $G_{\text{eff}} = 2G_{\text{WC}}G_{\text{diamond}}/(G_{\text{WC}} + G_{\text{diamond}}) \approx 380$ GPa. This gives, for the diamond/tungsten-carbide contact, $\tau \approx G_{\text{eff}}/1600$. The shear strength of this system is thus far below the ideal material shear strength [34,35]. Previous AFM results of Carpick et al. [3,6] and Lantz et al. [4] observed shear strengths near the ideal limit. An ideal shear strength in the range of $G/30$ suggests a "crystalline" or commensurate interface that is free of dislocations, where the commensurability may be brought about by atomic displacements induced by interfacial forces. Our measured shear strength indicates that there may be very little atomic commensurability for the diamond/tungsten-carbide interface, which is plausible considering the high stiffness of these materials. More importantly, the hydrogen passivation of the diamond surface strongly reduces the adhesive force, and also the friction force. In fact, removal of the hydrogen passivation would result in a value for the shear strength which is much larger than the ideal theoretical prediction of $G/30$ [22].

5. Conclusion

In conclusion, we have studied the nanotribological behavior of a well-defined hydrogen-terminated diamond(111)/tungsten-carbide single-asperity contact in UHV as a function of applied load. Local contact conductance measurements showed no significant changes in the shape of $I-V$ curves for loads up to 1.7 μN, as expected from the proportionality between the current and the contact area, which provided us with a direct and independent way of measuring the area of contact. Current (contact area) versus load data for a variety of bias voltages could excellently be fitted by the DMT model, which is in agreement with the finding that $\mu = 0.02 < 0.1$. Using the DMT relation for contact area versus load, we found that for this ideal single-asperity contact, i.e., one of the hardest, stiffest known heterocontacts, involving materials of great tribological importance, friction is directly proportional to the contact area: $F_f = \tau A$, where $\tau = 238$ MPa for loads up to 12 nN.

Acknowledgement

RJAvdO acknowledges the support of the Netherlands Organization for Scientific Research (NWO). RWC acknowledges the support of the Natural Sciences and Engineering Research Council of Canada. This work was supported by the Director, Office of Energy Research, Office of Basic Energy Sciences, Materials Sciences Division,

of the US Department of Energy under contract No. DE-AC03-76SF00098. The authors thank Dr. P. Reinke for the loan of the diamond sample.

References

[1] D. Dowson, *History of Tribology* (Longman, London, 1998).
[2] J.A. Greenwood and J.B.P. Williamson, Proc. Roy. Soc. London Ser. A 295 (1966) 300.
[3] R.W. Carpick, N. Agraït, D.F. Ogletree and M. Salmeron, J. Vac. Sci. Technol. B 14 (1996) 1289.
[4] M.A. Lantz, S.J. O'Shea, M.E. Welland and K.L. Johnson, Phys. Rev. B 55 (1997) 10776;
M.A. Lantz, S.J. O'Shea and M.E. Welland, Phys. Rev. B 56 (1997) 15345.
[5] M. Enachescu, R.J.A. van den Oetelaar, R.W. Carpick, D.F. Ogletree, C.F.J. Flipse and M. Salmeron, Phys. Rev. Lett. 81 (1998) 1877.
[6] R.W. Carpick, M. Enachescu, D.F. Ogletree and M. Salmeron, in: *Fracture and Ductile versus Brittle Behavior: Theory, Modeling, and Experiment*, Proceedings of the MRS Fall Meeting, Boston, 1998, eds. G. Beltz, K.-S. Kim and M. Marder.
[7] K.L. Johnson, K. Kendall and A.D. Roberts, Proc. Roy. Soc. London Ser. A 324 (1971) 301.
[8] D. Maugis, J. Colloid Interface Sci. 150 (1992) 243;
K.L. Johnson, Proc. Roy. Soc. London Ser. A 453 (1997) 163.
[9] B.V. Derjaguin, V.M. Müller and Y.P. Toporov, J. Colloid Interface Sci. 53 (1975) 314;
V.M. Müller, B.V. Derjaguin and Y.P. Toporov, Colloids Surf. 7 (1983) 251.
[10] H. Seki, G.M. McClelland and D.C. Bullock, Wear 116 (1987) 381; H. Tsai and D.B. Bogy, J. Vac. Sci. Technol. A 5 (1987) 3287.
[11] M.M. Schwartz, *Ceramic Joining* (ASM International, Materials Park, 1990).
[12] A.M. Homola, J.N. Israelachvili, M.L. Gee and P.M. McGuiggan, J. Tribol. 111 (1989) 675.
[13] K.L. Johnson, *Contact Mechanics* (Cambridge University Press, Cambridge, 1987).
[14] V.M. Müller, V.S. Yushenko and B.V. Derjaguin, J. Colloid Interface Sci. 77 (1980) 91.
[15] D. Tabor, J. Colloid Interface Sci. 58 (1977) 2;
K.L. Johnson, Langmuir 12 (1996) 4510.
[16] J.A. Greenwood, Proc. Roy. Soc. London Ser. A 453 (1997) 1277.
[17] A.G.M. Jansen, A.P. van Gelder and P. Wyder, J. Phys. C 13 (1980) 6073.
[18] S.M. Sze, *Physics of Semiconductor Devices* (Wiley, New York, 1981).
[19] G. Rubio, N. Agraït and S. Vieira, Phys. Rev. Lett. 76 (1996) 2303.
[20] M.N. Gardos, in: *Synthetic Diamond: Emerging CVD Science and Technology*, eds. K.E. Spear and J.P. Dismukes (Wiley, New York, 1994) p. 419.
[21] Q. Dai, R. Vollmer, R.W. Carpick, D.F. Ogletree and M. Salmeron, Rev. Sci. Instrum. 66 (1995) 5266.
[22] R.J.A. van den Oetelaar and C.F.J. Flipse, Surf. Sci. 384 (1997) L828.
[23] NT-MDT Co., Moscow, Russia.
[24] D.F. Ogletree, R.W. Carpick and M. Salmeron, Rev. Sci. Instrum. 67 (1996) 3298.
[25] J. Hu, X.-D. Xiao, D.F. Ogletree and M. Salmeron, Surf. Sci. 327 (1995) 358.
[26] F. Atamny and A. Baiker, Surf. Sci. 323 (1995) L314.
[27] S.S. Sheiko, M. Möller, E.M.C.M. Reuvekamp and H.W. Zandbergen, Phys. Rev. B 48 (1993) 5675.
[28] C.A. Klein, Mater. Res. Bull. 27 (1992) 1407.
[29] J.F. Shackelford, W. Alexander and J.S. Park, eds., *CRC Materials Science and Engineering Handbook* (CRC Press, Boca Raton, 1994).
[30] R.W. Carpick and M. Salmeron, Chem. Rev. 97 (1997) 1163, and references therein.
[31] R.W. Carpick, Q. Dai, D.F. Ogletree and M. Salmeron, Tribol. Lett. 5 (1998) 91.
[32] E. Barrena, S. Kopta, D.F. Ogletree, D.H. Charych and M. Salmeron, Phys. Rev. Lett. 82 (1999) 2880.
[33] A.H. Cottrell, *Introduction to the Modern Theory of Metals* (Institute of Metals, Brookfield, 1988).
[34] J. Hurtado and K.-S. Kim, Proc. Roy. Soc. London Ser. A, in press.
[35] J. Hurtado and K.-S. Kim, in: *Fracture and Ductile versus Brittle Behavior: Theory, Modeling, and Experiment*, Proceedings of the MRS Fall Meeting, Boston, 1998, eds. G. Beltz, K.-S. Kim and M. Marder.